Electronic Supplementary Material (ESI) for Journal of Analytical Atomic Spectrometry.

Strontium isotopic analysis of environmental microsamples by inductively coupled plasma - tandem mass spectrometry

Stefano Bertinetti, [a] Eduardo Bolea-Fernandez, [b] Mery Malandrino, [c] Beatrice Moroni, [d] David Cappelletti, [d] Marco Grotti [a] and Frank Vanhaecke [b]

[a] Department of Chemistry and Industrial Chemistry, University of Genoa, Via Dodecaneso 31, 16146 Genoa, Italy;

[b] Ghent University, Department of Chemistry, Atomic & Mass Spectrometry – A&MS – research group, Campus Sterre, Krijgslaan 281-S12, 9000, Ghent, Belgium;

[c] Department of Chemistry, University of Turin, Via Pietro Giuria 5, 10125, Turin, Italy;

[d] Department of Chemistry, Biology and Biotechnology, University of Perugia, 06123 Perugia, Italy.

Supplementary materials

Table S1. Experimental matrix (coded value) and experimental plan (real value).

	Coded value				Real value*			
Run	SD	UR	NG	MG	SD	UR	NG	MG
1	1	1	1	1	8	35	0.80	0.80
2	-1	1	1	1	4	35	0.80	0.80
3	1	-1	1	1	8	5	0.80	0.80
4	-1	-1	1	1	4	5	0.80	0.80
5	1	1	-1	1	8	35	0.20	0.80
6	-1	1	-1	1	4	35	0.20	0.80
7	1	-1	-1	1	8	5	0.20	0.80
8	-1	-1	-1	1	4	5	0.20	0.80
9	1	1	1	-1	8	35	0.80	0.40
10	-1	1	1	-1	4	35	0.80	0.40
11	1	-1	1	-1	8	5	0.80	0.40
12	-1	-1	1	-1	4	5	0.80	0.40
13	1	1	-1	-1	8	35	0.20	0.40
14	-1	1	-1	-1	4	35	0.20	0.40
15	1	-1	-1	-1	8	5	0.20	0.40
16	-1	-1	-1	-1	4	5	0.20	0.40
17	1	0	0	0	8	20	0.50	0.60
18	-1	0	0	0	4	20	0.50	0.60
19	0	1	0	0	6	35	0.50	0.60
20	0	-1	0	0	6	5	0.50	0.60
21	0	0	1	0	6	20	0.80	0.60
22	0	0	-1	0	6	20	0.20	0.60
23	0	0	0	1	6	20	0.50	0.80
24	0	0	0	-1	6	20	0.50	0.40
25-30	0	0	0	0	6	20	0.50	0.60

Note: * SD = Plasma sampling depth (mm); UR = sample uptake rate (µL min^{-1}); NG = nebulizer gas flow rate (L min^{-1}); MG = make-up gas flow rate (L min^{-1}).

Table S2. Coefficients of the model for the $^{86}SrF^{+}$ ion intensity and their significance.

Coefficient	Factor	Value	Significance
b0	mean	65070	$p < 0.01$
b1	SD	-10230	$p = 0.08$
b2	UR	11766	$p < 0.05$
b3	NG	10685	$p = 0.07$
b4	MG	-6456	$p = 0.26$
b5	SD*UR	-1760	$p = 0.77$
b6	SD*NG	-2198	$p = 0.71$
b7	SD*MG	2847	$p = 0.63$
b8	UR*NG	6202	$p = 0.30$
b9	UR*MG	-5905	$p = 0.33$
b10	NG*MG	-20596	$p < 0.01$
b11	SD*SD	26542	$p = 0.09$
b12	UR*UR	-6008	$p = 0.68$
b13	NG*NG	-46142	$p < 0.01$
b14	MG*MG	-18962	$p = 0.21$

Table S3. Coefficients of the model for the precision (RSD%) of the $^{86}SrF^{+}$ ion intensity and their significance.

Coefficient	Factor	Value	Significance
b0	mean	2.44	$p < 0.001$
b1	SD	-0.50	$p = 0.15$
b2	UR	-1.79	$p < 0.001$
b3	NG	-1.24	$p < 0.01$
b4	MG	-0.09	$p = 0.79$
b5	SD*UR	0.37	$p = 0.32$
b6	SD*NG	0.27	$p = 0.45$
b7	SD*MG	0.04	$p = 0.91$
b8	UR*NG	1.53	$p < 0.001$
b9	UR*MG	0.81	$p < 0.05$
b10	NG*MG	0.97	$p < 0.05$
b11	SD*SD	0.33	$p = 0.71$
b12	UR*UR	1.69	$p = 0.07$
b13	NG*NG	0.86	$p = 0.34$
b14	MG*MG	-0.22	$p = 0.80$

Table S4. Coefficients of the model for the $^{87}Sr/^{86}Sr$ precision (RSD%) and their significance.

Coefficient	Factor	Value	Significance
b0	mean	0.15	$p < 0.05$
b1	SD	-0.08	$p = 0.13$
b2	UR	-0.08	$p = 0.09$
b3	NG	-0.15	$p < 0.01$
b4	MG	-0.07	$p = 0.18$
b5	SD*UR	0.10	$p = 0.07$
b6	SD*NG	-0.21	$p < 0.001$
b7	SD*MG	-0.21	$p < 0.001$
b8	UR*NG	-0.02	$p = 0.74$
b9	UR*MG	0	$p = 0.99$
b10	NG*MG	0.62	$p < 0.001$
b11	SD*SD	0.07	$p = 0.61$
b12	UR*UR	0.07	$p = 0.61$
b13	NG*NG	0.49	$p < 0.005$
b14	MG*MG	0.13	$p = 0.29$

Table S5. Coefficients of the model for the $^{88}Sr/^{86}Sr$ precision (RSD%) and their significance.

Coefficient	Factor	Value	Significance
b0	mean	0.30	$p < 0.005$
b1	SD	-0.14	$p < 0.05$
b2	UR	0.04	$p = 0.50$
b3	NG	-0.06	$p = 0.34$
b4	MG	-0.05	$p = 0.38$
b5	SD*UR	-0.09	$p = 0.20$
b6	SD*NG	-0.24	$p < 0.005$
b7	SD*MG	-0.20	$p < 0.01$
b8	UR*NG	-0.06	$p = 0.37$
b9	UR*MG	-0.07	$p = 0.31$
b10	NG*MG	0.60	$p < 0.001$
b11	SD*SD	-0.13	$p = 0.41$
b12	UR*UR	0.03	$p = 0.84$
b13	NG*NG	0.52	$p < 0.005$
b14	MG*MG	0.29	$p = 0.09$

Table S6. Validation results. The experiments were conducted with the selected parameters: SD = 4 mm, UR = 20 µL min^{-1}, NG = 0.57 L min^{-1}, MG = 0.50 L min^{-1}.

	Predicted value$^{\sharp}$	**SD***	**Experimental value**$^{\sharp}$	**SD***
$^{86}SrF^{+}$	104664	1684	111775	2489
RSD%87/86	0.22	0.04	0.15	0.06
RSD%88/86	0.31	0.07	0.31	0.11
$^{87}Sr/^{86}Sr$	0.7139	0.0008	0.7147	0.0012

Note: ♯ the values correspond to the 5-fold repetition of the analysis of 10 ng g^{-1} Sr standard solution; * uncertainty as the standard deviation.

Table S7. Coefficients of the model for the $^{87}Sr/^{86}Sr$ isotope ratio and their significance.

Coefficient	Factor	Value	Significance
b0	mean	0.7161	$p < 0.001$
b1	SD	0.0008	$p = 0.20$
b2	UR	0.0009	$p = 0.13$
b3	NG	-0.0033	$p < 0.001$
b4	MG	-0.0018	$p < 0.01$
b5	SD*UR	-0.0006	$p = 0.33$
b6	SD*NG	0.0015	$p < 0.05$
b7	SD*MG	0.0017	$p < 0.05$
b8	UR*NG	-0.0004	$p = 0.53$
b9	UR*MG	-0.0002	$p = 0.78$
b10	NG*MG	-0.0015	$p < 0.05$
b11	SD*SD	-0.0024	$p = 0.13$
b12	UR*UR	-0.0024	$p = 0.14$
b13	NG*NG	0.0022	$p = 0.18$
b14	MG*MG	0.0005	$p = 0.76$

Table S8. $^{87}Sr/^{86}Sr$ isotope ratios and their uncertainties for the two types of soil samples (*non- grinded* and *grinded*) from Australia and South America.

Sample	$^{87}Sr/^{86}Sr$	±u (α=0.05)	coordinates
Australia – non-grinded			
AUS 1	0.7148	0.0006	S12° 51.732' E132° 47.724'
AUS 14	0.7125	0.0023	S18° 56.806' E134° 7.546'
AUS 26	0.7291	0.0016	S23° 37.803' E133° 52.191'
AUS 36 B	0.7180	0.0011	S25° 22.609' E133° 11.529'
AUS 53	0.7151	0.0017	S31° 22.051' E136° 54.044'
Australia – grinded			
AUS 1	0.7159	0.0008	S12° 51.732' E132° 47.724'
AUS 14	0.7277	0.0011	S18° 56.806' E134° 7.546'
AUS 26	0.7248	0.0012	S23° 37.803' E133° 52.191'
AUS 36 A	0.7246	0.0004	S25° 22.609' E133° 11.529'
AUS 36 B	0.7191	0.0008	S25° 22.609' E133° 11.529'
AUS 53	0.7144	0.0011	S31° 22.051' E136° 54.044'
South America – non-grinded			
PAT 1	0.7090	0.0015	S31° 47.826' W65° 07.071'
PAT 4	0.7204	0.0015	S32° 28.764' W66° 56.899'
PAT 12 A	0.7054	0.0022	S39° 07.117' W67° 41.211'
PAT27 A	0.7063	0.0017	S37° 13.718' W70° 14.319'
South America – grinded			
PAT 4	0.7191	0.0010	S32° 28.764' W66° 56.899'
PAT 12 A	0.7081	0.0005	S39° 07.117' W67° 41.211'
PAT 12 B	0.7068	0.0008	S39° 07.117' W67° 41.211'
PAT 27 A	0.7076	0.0010	S37° 13.718' W70° 14.319'
PAT 27 B	0.7070	0.0008	S37° 13.718' W70° 14.319'

Table S9. $^{87}Sr/^{86}Sr$ isotope ratios and their uncertainties for the Antarctic PM_{10} samples and their insoluble fractions. The samples were collected at the Concordia research station, in East Antarctica, during 2018.

Sample	$^{87}Sr/^{86}Sr$	±u (α=0.05)	Sampling period
	PM10 DC – Total		
DC_1_18	0.7066	0.0008	10/12/2017 → 23/01/2018
DC_2_18	0.7083	0.0013	23/01/2018 → 23/02/2018
DC_3_18	0.7102	0.0012	23/02/2018 → 21/03/2018
DC_4_18	0.7049	0.0012	21/03/2018 → 20/04/2018
DC_5_18	0.7076	0.0009	20/04/2018 → 20/05/2018
DC_6_18	0.7080	0.0011	20/05/2018 → 21/06/2018
DC_7_18_A	0.7074	0.0018	21/06/2018 → 10/07/2018
DC_7_18_B	0.7078	0.0005	10/07/2018 → 23/07/2018
DC_8_18	0.7076	0.0011	23/07/2018 → 22/08/2018
DC_9_18	0.7092	0.0007	22/08/2018 → 21/09/2018
DC_10_18	0.7089	0.0007	21/09/2018 → 23/10/2018
DC_11_18	0.7064	0.0015	23/10/2018 → 24/11/2018
DC_12_18	0.7067	0.0019	24/11/2018 →25/12/2018
	PM10 DC – Insoluble fraction		
DC_1_18	0.7079	0.0005	10/12/2017 → 23/01/2018
DC_2_18	0.7081	0.0016	23/01/2018 → 23/02/2018
DC_3_18	0.7079	0.0016	23/02/2018 → 21/03/2018
DC_4_18	0.7055	0.0011	21/03/2018 → 20/04/2018
DC_5_18	0.7067	0.0007	20/04/2018 → 20/05/2018
DC_6_18	0.7090	0.0014	20/05/2018 → 21/06/2018
DC_7_18_A	0.7063	0.0012	21/06/2018 → 10/07/2018
DC_7_18_B	0.7063	0.0013	10/07/2018 → 23/07/2018
DC_8_18	0.7075	0.0013	23/07/2018 → 22/08/2018
DC_9_18	0.7066	0.0023	22/08/2018 → 21/09/2018
DC_10_18	0.7082	0.0017	21/09/2018 → 23/10/2018
DC_11_18	0.7066	0.0020	23/10/2018 → 24/11/2018
DC_12_18	0.7074	0.0015	24/11/2018 →25/12/2018

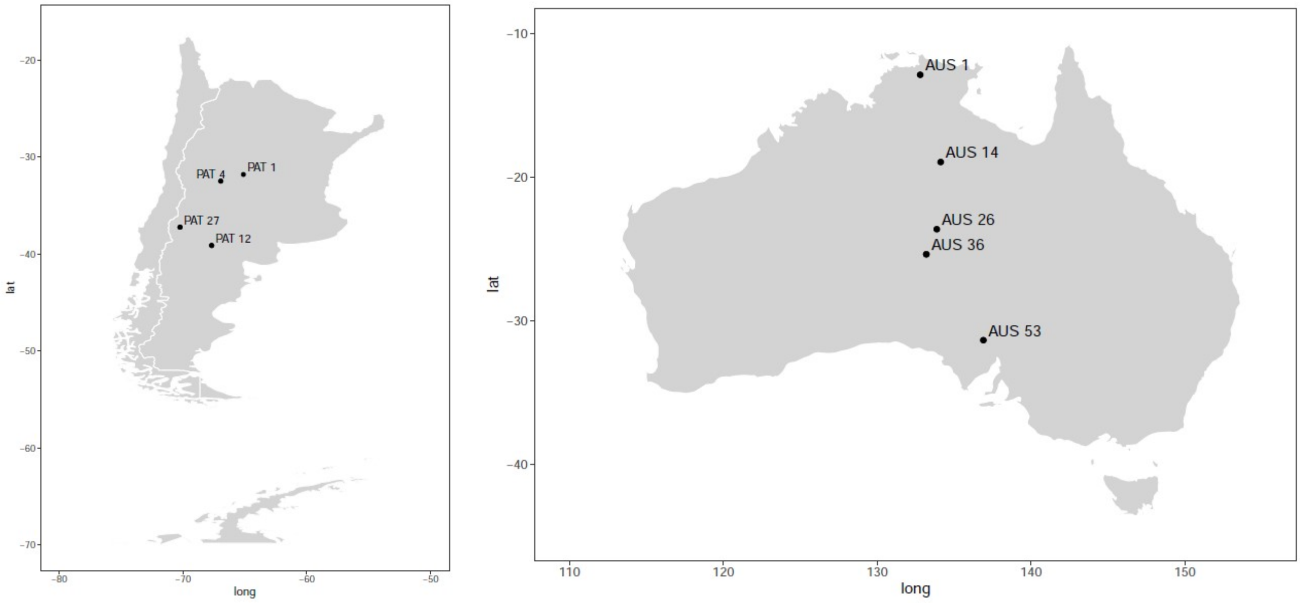

(a) (b)

Figure S1. Sampling sites for (a) South American and (b) Australian soil samples.

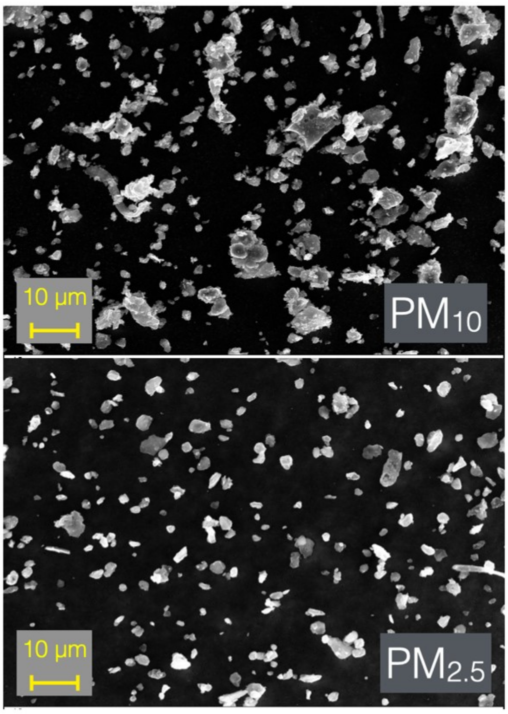

Figure S2. SEM images (obtained using 15 keV electrons and magnification 2.5x) of resuspended material of an Australian dust sample (AUS5) not grinded and deposited on polycarbonate filter, using either a PM_{10} or a $PM_{2.5}$ impactor head.

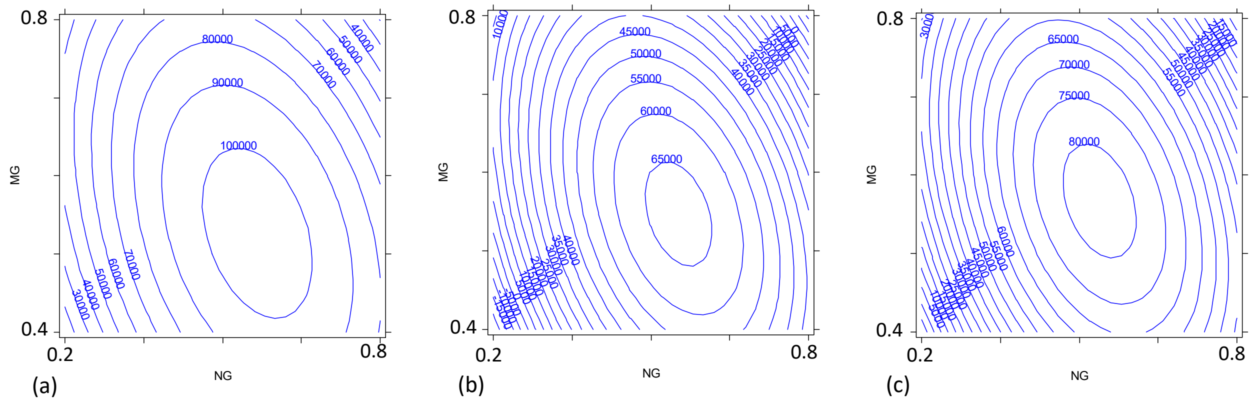

Figure S3. Combined effect of the nebulizer gas flow rate (NG, L min^{-1}) and make-up gas flow rate (MG, L min^{-1}) on the $^{86}SrF^{+}$ signal intensity for the sampling depth (SD) set at (a) 4 mm, (b) 6 mm and (c) 8 mm (UR = 35 µL min^{-1}).

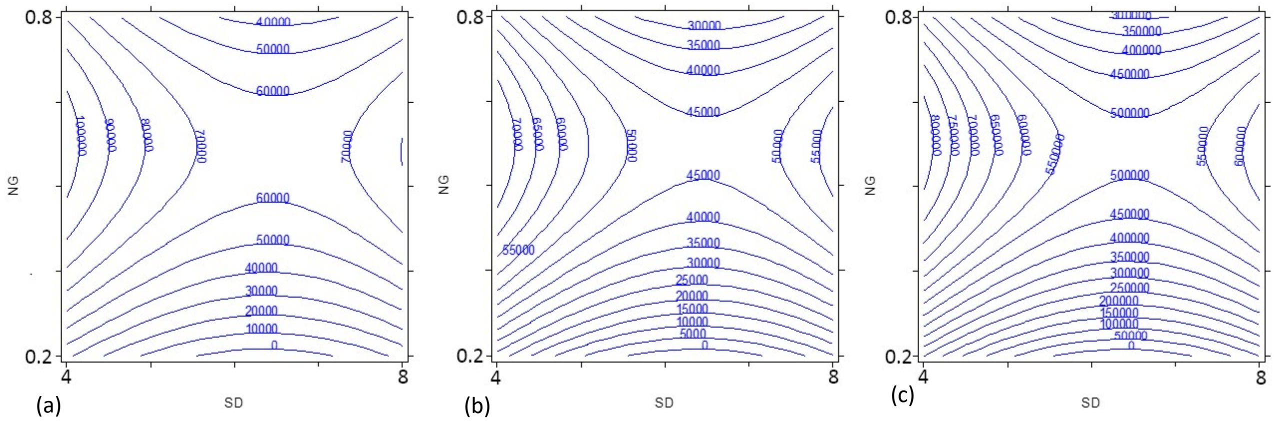

Figure S4. Combined effect of the nebulizer gas flow rate (NG, L min^{-1}) and plasma sampling distance (SD, mm) on the intensity for the ions (a) $^{86}SrF^{+}$, (b) $^{87}SrF^{+}$ and (c) $^{88}SrF^{+}$ (UR= 20 µL min^{-1}; MG = 0.50 L min^{-1}).

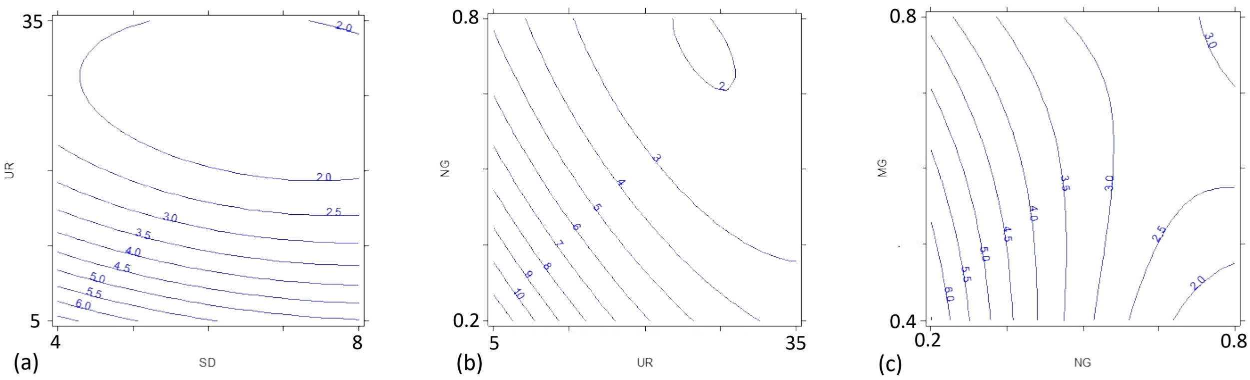

Figure S5. Combined effect of the sample uptake rate (UR, µL min^{-1}), nebulizer gas flow rate (NG, L min^{-1}), plasma sampling distance (SD, mm) and make-up gas flow rate (MG, L min^{-1}) on the precision (RSD%) of the signal for the $^{86}SrF^{+}$ ion. (a) NG = 0.57 L min^{-1}, MG= 0.50 L min^{-1}; (b) SD = 4 mm, MG = 0.50 L min^{-1}; (c) UR = 20 µL min^{-1}, SD = 4 mm.

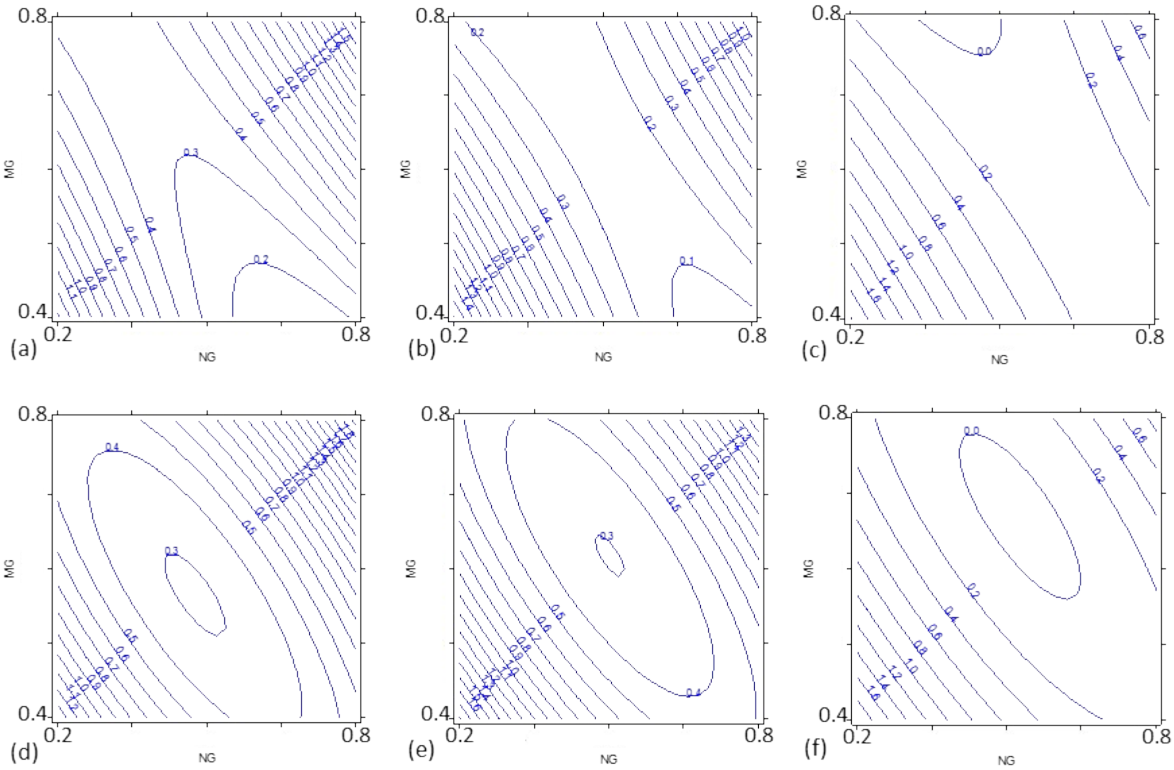

Figure S6. Combined effect of the nebulizer gas flow rate (NG, L min^{-1}) and make-up gas flow rate (MG, L min^{-1}) on the precision (RSD%) of the $^{87}Sr/^{86}Sr$ (contour plots a-b-c) and $^{88}Sr/^{86}Sr$ (contour plots d-e-f) isotope ratios. SD are set at 4 mm (a and d), 6 mm (b and e), and 8 mm (c and f) (UR = 20 µL min^{-1} for each graph).